

This is the final peer-reviewed accepted manuscript of:

R. Men *et al.* Effect of thermal ageing on space charge in ethylene propylene rubber at DC voltage

in *IEEE Transactions on Dielectrics and Electrical Insulation*, vol. 26, no. 3, pp. 792-800, June 2019

The final published version is available online at: <https://doi.org/10.1109/TDEI.2018.007752>

Rights / License:

The terms and conditions for the reuse of this version of the manuscript are specified in the publishing policy. For all terms of use and more information see the publisher's website.

This item was downloaded from IRIS Università di Bologna (<https://cris.unibo.it/>)

When citing, please refer to the published version.

Effect of Thermal Ageing on Space Charge in Ethylene Propylene Rubber at DC Voltage

Rujia Men, Zhipeng Lei^{1,2}, Jiancheng Song, Yuanyuan Li, Lingyan Lin and Muqin Tian

¹Shanxi Key Laboratory of Mining Electrical Equipment and Intelligent Control, National & Province Joint Engineering Laboratory of Intelligent Electrical Apparatus, College of Electrical and Power Engineering, Taiyuan University of Technology
Taiyuan, Shanxi 030024, China

Davide Fabiani

²Department of Electrical, Electronic and Information Engineering 'G. Marconi', University of Bologna
Bologna 40134, Italy

Xiaoxiao Xu

³State Grid Hebei Maintenance Branch of China
Shijiazhuang, Hebei 050000, China

ABSTRACT

To understand the space charge characteristics of ethylene propylene rubber (EPR) used in MV/HV power cables under thermal stress, the space charge profile is measured by the pulsed electro-acoustic method under 20 kV/mm at 120 and 160 °C. The complex permittivity and physicochemical properties at the different ageing stages are measured and analyzed for an understanding of the effects of thermal ageing on space charge characteristics. The trap properties of EPR during thermal ageing is calculated and analyzed based on the space charge decay model. The results show that both the ageing time and temperature can affect the space charge characteristics of EPR. The space charge characteristics of EPR can be ascribed to the trapping sites caused by the complex chemical and physical structures during thermal ageing. Under the thermal oxygen process, the polar groups and ions increase because of the EPR molecular chain breakages, and the charge injection from the electrodes increases. Based on the decay model of space charge and isothermal decay current theory, the distribution of trap levels in EPR at different ageing stages is obtained. The trap distribution under different ageing process can be explained by the theory of trap filling.

Index Terms — ethylene propylene rubber, space charge, thermal ageing, dielectric temperature spectrum, trap level

1 INTRODUCTION

ETHYLENE propylene rubber (EPR), being of excellent moisture resistance, thermal resistance, corona resistance and high tensile strength, has been widely used as the insulating material of MV/HV power cables and accessories. Its corrosion resistance, flexibility and dielectric properties are further enhanced after vulcanization [1,2]. With the improvement of voltage level and the study on the ageing of polymer dielectric, space charge has received a great deal of attention. Researchers have proven that the accumulation of space charge can directly distort the local electric field of dielectric materials and influence its insulation properties [1-4]. Moreover, since EPR was used as insulation material, the thermal stress has been thought as one of important factors

affecting the insulation properties. Under the thermal stress, irreversible physical-chemical processes occur in the polymer insulation [5, 6], which lead to a continuous worsening of the insulation properties. During this process, the space charge characteristics may change, and finally influence the insulation properties.

Considerable research has been done on the ageing and space charge of EPR in recent years. The space charge distribution was usually obtained by pulsed electro-acoustic (PEA) method [7-9], pressure wave propagation (PWP) method [10] or thermal step method (TSM) [11]. Considering the different applications of EPR such as HVDC joints and HV cable, the ageing condition were commonly set as a single factor [10, 12, 13] or a multifactor [14, 15]. The specific research work mainly includes the following parts. In [16], the

space charge distribution in EPR and XLPE were measured under thermal gradient, which reveals the field distortion were enhanced with the thermal gradient. In [17], the space charge characteristics of interface between EPR and LDPE under different surface state controlled by the fluorination time were studied, the results show that the fluorination can effectively suppress the interface charge. In [18], the effect of electric stress on the space charge characteristics of EPDM was studied by measuring and analyzing the space charge distribution and conduction current simultaneously, which reveals the energy loss dynamics caused by space charge. In [19], the electrical conductivity and permittivity were measured and supported the increase of the ionic dipoles during ageing process. Besides, the related physicochemical parameters were measured during ageing. In [17], the FTIR spectroscopy was used for clarifying the characterization of the material degradation by oxidation during thermal ageing.

Most researches on the space charge characteristics of aged EPR, especially under thermal ageing, have been aimed at the application as composites and comparing the space charge characteristics with other polymer insulation. However, the researches on the long-term ageing properties of EPR and the effects on the space charge characteristics are relatively rare. In the paper, the samples have been thermally aged at different temperature. The space charge profile under polarization and depolarization has been measured at the different ageing stages. The charge quantity and trap levels have been analyzed. The cross sections of EPR at different ageing stages has been studied. The change of molecular structure has also been analyzed for clarifying the physicochemical properties during ageing, and the permittivity were used for the analysis of dielectric properties during ageing.

2 EXPERIMENTAL SETUP

2.1 SAMPLE PREPARATION

The DCJ30M type EPR, mixed and filtered in the manufactory, was vulcanized for 15 min under 160 °C and 14 MPa in laboratory. The cured samples were naturally cooled down to room temperature and then immediately put into the vacuum drying oven with 80 °C and 50 Pa for 24 hours in order to eliminate the possible by-product and mechanical stress during vulcanization. Finally, the samples with a thickness of 390 μm were cut into discs with a diameter of 60 mm.

2.2 THERMAL AGEING EXPERIMENT

The thermal ageing tests were conducted in an electro-thermostatic blast oven. The ageing temperature were 120 °C and 160 °C. The time points of space charge measurement were shown in Table.1. At each time point, the samples were taken from the blast oven and cooled down to room temperature. Then the space charge profile during polarization for 30 min and depolarization for 60 min, as well as the dielectric spectrum, were measured. During the measurement of PEA and the dielectric spectrum, the separate samples aged together at the same condition were used. It should be noted

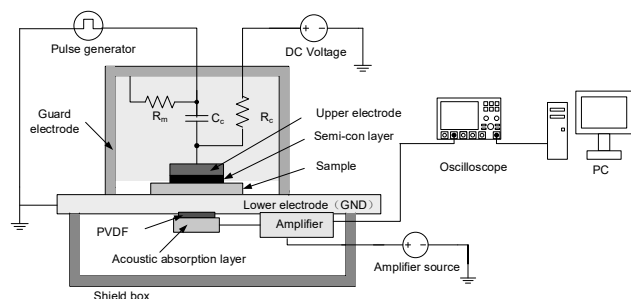
that only some characteristic stages of the space charge profile, including 8, 30, 60, 120 days at the ageing temperature of 120 °C, and 2, 4 days at 160 °C, are shown in the paper.

Table 1. Time points of space charge measurement.

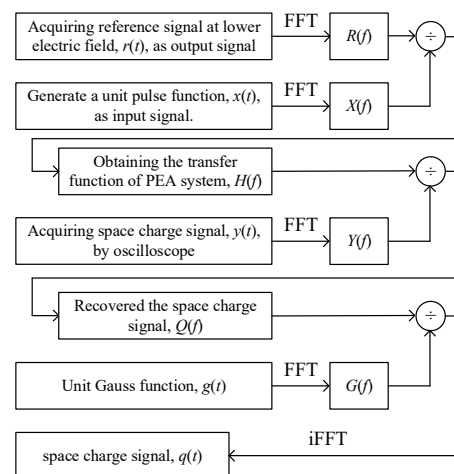
Ageing temperature/°C	total ageing time/days	Time points of measurement/days
120	125	0, 4, 8, 20, 30, 400, 50, 60, 70, 80, 90, 100, 110, 120
140	40	0, 2, 4, 8, 20, 30, 40
160	6	0, 2, 4

2.3 SPACE CHARGE MEASUREMENT

The space charge was measured by the PEA method, Peanuts Five Lab, as shown in Figure 1. The measurement sensitivity of PEA device is about 0.2 C/m³, and also depends on the sample. In the paper, the peak of space charge is analyzed when the charge density is about 5 times larger than the measurement sensitivity of PEA device. The upper and lower electrodes of the test device were semiconductor layer (SC) and aluminum (Al) respectively. The pulse voltage during the experiment was 400 V. The space charge profile of each ageing stage was measured under 20 kV/mm (Al is anode and SC is cathode) within 30 min. After that, the voltage was removed and the dissipation characteristics within 60 min were measured.



(a) experimental setup



(b) space charge data processing

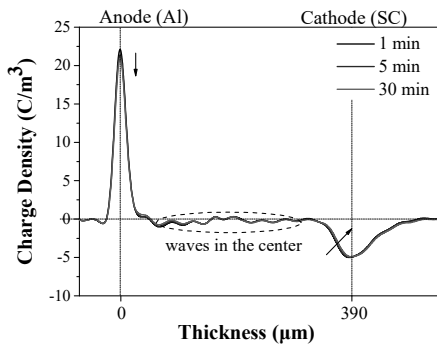
Figure 1. Schematic diagram of PEA technique.

Generally, there are some waves in the center part of space charge profiles as shown in Figure 2, because Gauss filter is used to process signal after the recovery of space charge profile by Takada's method [20] as shown in Figure 1b. Firstly, in order to obtain the transfer function of PEA device, the reference signal was acquired at electric field which was lower and short enough to avoid space charge accumulation in the sample during volt-on. Secondly, the recovered space charge signal could be obtained by the twice deconvolution operation in time domain which was equal to the division operation in frequency domain. Then, the Gauss function was used to filter the recovered space charge signal. Finally, space charge distribution in time domain could be obtained by inverse fast Fourier transform (iFFT).

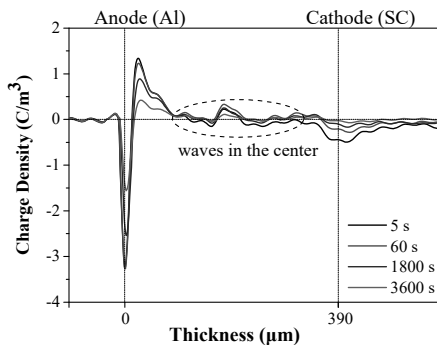
The amount of wave in space charge profiles depends on the value of σ , the full width at half maximum of the peak in Gauss function, $g(x)$, expressed as:

$$g(x) = \frac{1}{\sigma\sqrt{2\pi}} \exp\left[-\left(\frac{x-\mu}{\sqrt{2}\sigma}\right)^2\right] \quad (1)$$

where μ is the position of the center of the peak, and x is the data acquired in the time domain. If the value of σ increases, the profile will be smooth, but the peak magnitude decreases. However, if the value of σ is small, the wave will rise and the space charge profile can't be analyzed.



(a) polarization



(b) depolarization

Figure 2. Space charge profile of un-aged EPR sample.

2.4 DIELECTRIC SPECTRA AND SEM

Dielectric properties of EPR in the paper were measured by Novocontrol Concept 80. Relative permittivity was measured

at 1 V with frequency of 0.01~10⁶ Hz. The error of the measuring instrument was within 2%. After the samples were fractured in liquid nitrogen, the cross sections of EPR was studied by TESCAN VEGA3SB SEM for clarifying the physical change during thermal ageing.

3 RESULTS

3.1 SPACE CHARGE PROFILE UNDER POLARIZATION

Generally, the accumulated space charge in the bulk is often classified into homocharge and heterocharge, based on the polarity of charge and adjacent electrode. Homocharge refers to the polarity of space charge same to that of adjacent electrode, and the heterocharge is the reverse situation. It should be noted that the two dotted lines in the figure of space charge profile represent the location of anode (Al) and cathode (SC) respectively in the paper. The relationship between the charge density of interface, σ , and the space charge density near the electrodes, $\rho(z)$, can be expressed as:

$$\sigma = \epsilon_r \epsilon_0 E_{av} - \int_0^d \rho(z) dz \quad (2)$$

where ϵ_0 and ϵ_r are the vacuum permittivity and relative permittivity respectively, E_{av} is the applied average electric field, d is the thickness of the sample. According to equation above, the increase of homocharge or the decrease of heterocharge near the electrodes will make the interface charge density decrease. On the contrary, the decrease of homocharge or the increase of heterocharge near the electrodes will make the interface charge density increase.

The space charge profile of un-aged EPR samples during polarization and depolarization are shown in Figure 2. In Figure 2a, the space charge density of the interface between the anode and sample decreases with time. When the voltage is removed, it can be found in Figure 2b that the homocharge accumulates in the vicinity of anode, and the polarity of the induced charge at the interface changes is negative, which means that the charge is injected from the anode in poling process. As shown in Figure 2a, the space charge density of the interface between the cathode and sample is nearly invariable. The charge peak at the cathode has a slight offset away from the sample, which means that a little of heterocharge appears near the cathode, and a part of electron injected from the cathode may be neutralized by these heterocharge. When the voltage is removed, the space charge near the cathode dissipates fast.

The space charge profile of EPR during 120 °C ageing is presented in Figure 3. It is shown in Figure 3a that the space charge near the anode becomes heterocharge when the sample is aged for 8 days. In Figure 3b, it can be seen that the space charge near the anode changes back to homocharge when the sample is aged for 30 days, and the similar phenomena can be observed until the end life of EPR. Generally, charge injection is thought as the source of homocharge. The dissociation of impurities and migration of injected charge are the main source of the heterocharge. The presence of heterocharge near

two electrodes at the early stage of thermal ageing, about less than 30 days, is regarded as “re-degassing process”. The re-degassing process will cause the dissociation and evaporation of the impurities [13], and increase the heterocharge near the anode which neutralizes the injected positive charge from the

anode. When the sample is aged more than 30 days, the charge injection from the anode will dominate, which results in homocharge accumulation near the anode.

It is noteworthy to observe in Figure 3b and 3c that the decline rate of maximum interface charge density from 1 min to 30 min at the anode increases with ageing time. The maximum interface charge density declines 2.5 and 7.1 C/m^3 , respectively, which means the charge injection is more easily from the anode based on Equation (1). As shown in Figure 3d, the maximum interface charge density at the anode after aged for 120 days declines 3.6 C/m^3 and is smaller than that aged for 60 days, which may be caused by the electrode injection and the electron neutralization.

The charge density of interface between the cathode and sample increases with ageing time at each ageing stage, which means that heterocharge begins to accumulate near the cathode during the ageing process. After poling for 30 min, the heterocharge density increases first, and reaches the maximum of about 2.2 C/m^3 when sample is aged 60 days. After 60 days, the heterocharge density near cathode decreases with ageing time. It can be inferred that although there is a certain amount of the charge injected from the cathode, the injected electron is neutralized by the positive space charge which migrates from the anode. The space charge density at the inner part of sample is still lower than that near the electrodes.

The space charge profile in EPR samples under 160 °C thermal ageing is presented in Figure 4. It is obviously that the life of EPR under 160 °C ageing is shorter than that under 120 °C, and the space charge profile under polarization is also different

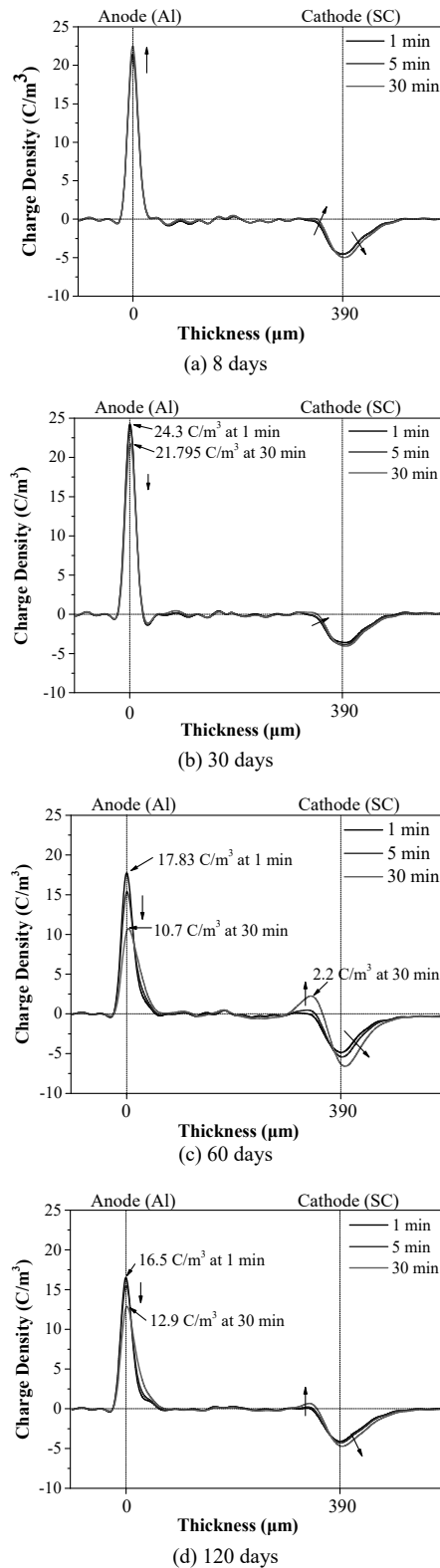


Figure 3. Space charge profile of EPR under polarization at different ageing stages of 120 °C.

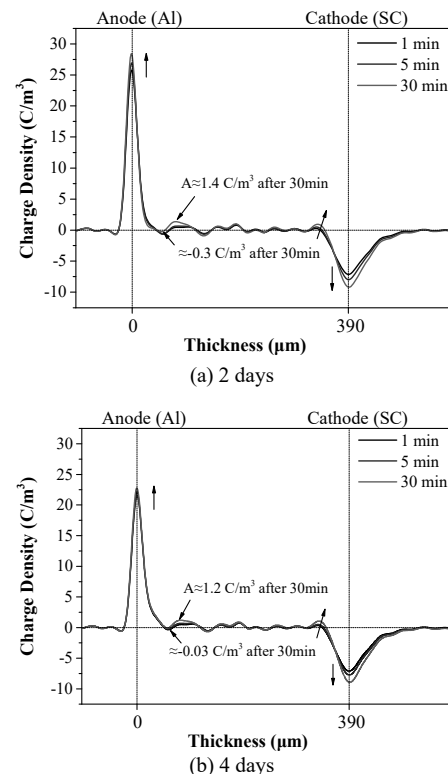


Figure 4. Space charge profile of EPR under polarization at different ageing stages of 160 °C.

from the results of 120 °C. Compared to un-aged samples, the charge density in the interfaces is increased with ageing time, which means that heterocharge accumulates near the cathode. Moreover, a little of positive charge accumulates inside the sample as shown in point A, and the density of negative charges accumulating on the front of A, decreases. It can be concluded that not only the ageing time but also the ageing temperature (or thermal ageing speed) has an influence on the space charge characteristics. In general, it can be seen from Figure 3 and Figure 4 that the homocharge in EPR mainly accumulates at two electrodes under polarization. The charge polarity near the anode will change during thermal ageing at 120 °C, then the positive charge injection will dominate and the depth of charge injection increases. A certain amount of heterocharge, which accumulates near the cathode, is affected by the thermal ageing extent.

3.2 DISSIPATION CHARACTERISTICS OF SPACE CHARGE IN EPR

The space charge profile during depolarization is shown in Figure 5. The space charge during depolarization can accurately reflect the migration of internal space charge, and is used to evaluate the change of the dielectric during thermal ageing.

In Figure 5, the polarity of space charge near the electrodes during depolarization is consistent with that during polarization, and the opposite charge is induced at the interfaces. Heterocharge is observed near the cathode, the charge density of which reaches the maximum when sample is aged for 60 days. It can be seen that the space charge of EPR aged for 60 days dissipates fast after the applied voltage is removed, especially in the initial 5 s. After 3600 s, there is a small amount of charge accumulating near the electrodes because of the bounds of deep traps. The change of space charge during depolarization can be described clearly by the charge quantity, $Q(t)$,

$$Q(t) = \int_0^d |\rho(x, t)| S dx \quad (3)$$

where d is the thickness of sample, S is the area of electrodes, $\rho(x, t)$ is the charge density at time, t , and within a certain thickness, x .

The decay profile can be fitted by a one-order exponential model

$$\sigma = \sigma_0 + K e^{-t/\tau} \quad (4)$$

where σ is the space charge density, σ_0 is final charge density, τ is the decay time constant.

The charge quantity of different ageing stages is shown in Figure 6. It can be seen that the space charge quantity decreases in a relatively rapid rate during the initial several hundred seconds and then slows down. The charge quantity increases first and decreases when the samples aged at 120 °C approaches to the end of life. The maximum charge quantity of sample aged at 160 °C increases with the ageing time. The dissipation of space charge is related to the trap distribution in EPR, which will be discussed later.

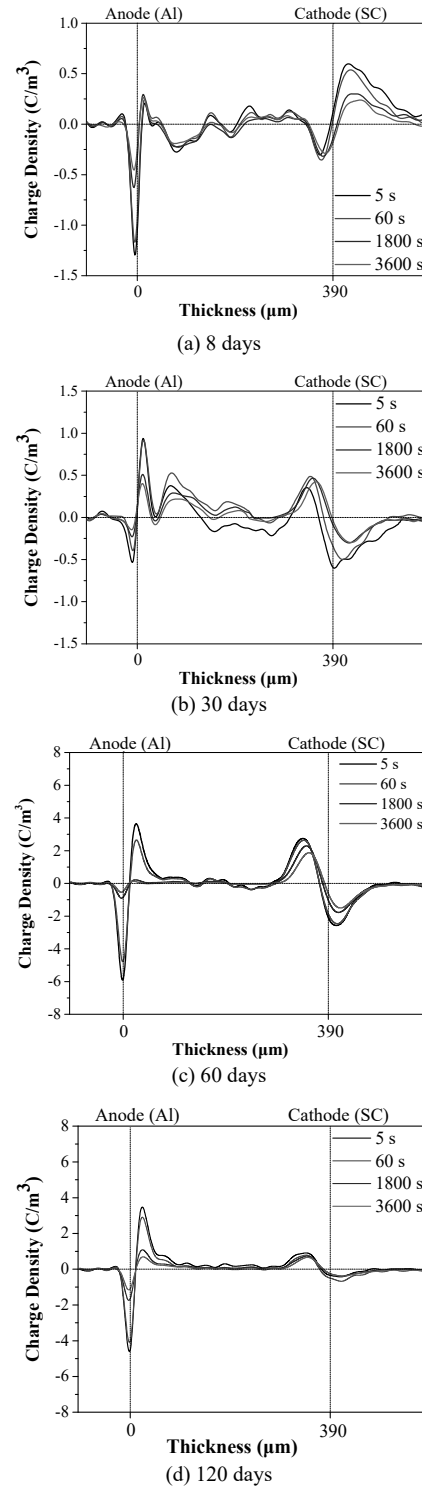


Figure 5. Space charge profile of EPR under depolarization at different ageing stages of 120 °C.

4 DISCUSSION

In this section, the trap level is calculated and analyzed for explaining the space charge characteristics during thermal ageing. The permittivity and physicochemical properties are also measured and analyzed for a further thoroughly understanding of the influence of the thermal stress on the space charge distribution in EPR.

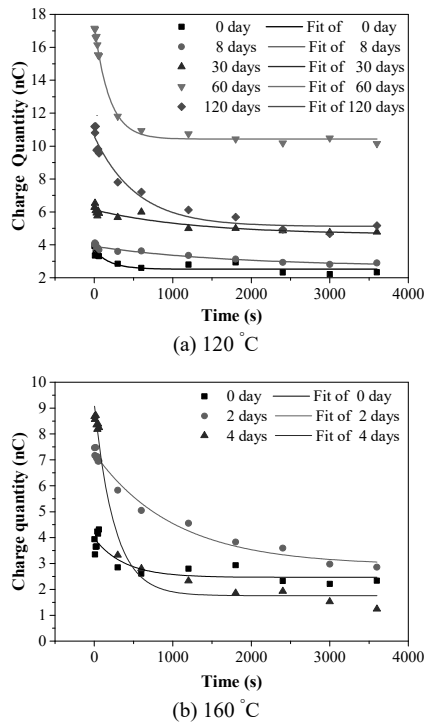


Figure 6. Charge quantity of space charge at different ageing temperature.

4.1 DIELECTRIC SPECTRUM

Clarifying the phenomenon of polarization and relaxation is main purpose of studying the dielectric properties, so the dielectric properties interrelated with the space charge characteristics[21]. The dielectric spectra of samples at each thermal ageing stage are shown in Figure 7. It can be observed that the real part of complex permittivity, ϵ' , and the imaginary part of complex permittivity, ϵ'' , increase at low frequency with ageing time. As for the reasons, on the one hand, the electrode polarization is the main reason which leads to the increase of ϵ' and ϵ'' . The conductivity will increase with the increase of carriers in the sample, the mobility of the carriers is small at low frequency, which makes the carriers accumulate

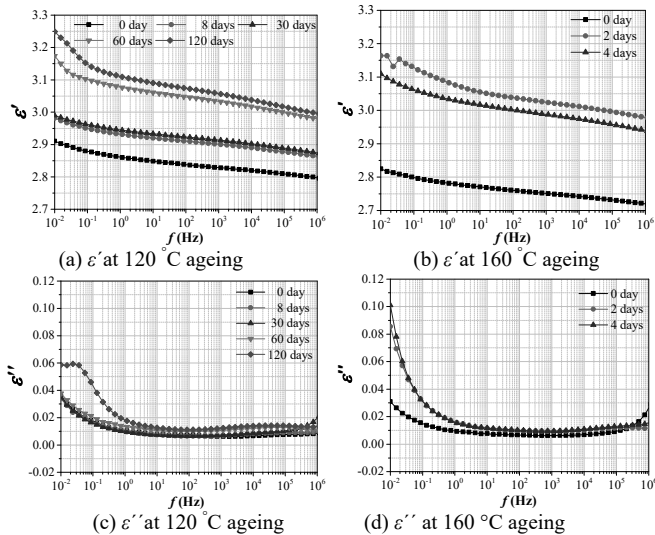


Figure 7. Complex permittivity of EPR aged at different temperature.

at the interface and forms the extra polarization and then makes the ϵ' and ϵ'' increase. On the other hand, the increase of ions will enhance the ionic polarization especially at low frequency. It proves that the thermal ageing causes the increase of dipolar groups, the enhancement of polarization and the increase of dielectric loss, which is consistent with the change of the profile of space charge.

4.2 PHYSICOCHEMICAL PROPERTIES DURING THERMAL AGEING

The cross section of EPR at different ageing states is showed in Figure 8. The surface of the un-aged EPR is characterized by the sparse and obvious wrinkles, which indicated that there was remarkable toughness fracture surface morphology. With the increase of ageing time, the roughness increases and then the wrinkles become dense as shown in Figure 8b. At the end of life of EPR, there are compact micropores and small holes on the surface as shown in Figure 8c and 8d. The change of physical properties of the cross section showed the deterioration of EPR under thermal ageing. According to these visible changes of the cross section of sample, it can be concluded that the high temperature increased the ageing rate of sample. It also can be deduced that the physical changes during thermal ageing can influence the distribution of traps and the density of carriers in the sample, and further affect the space charge distribution at different ageing stage.

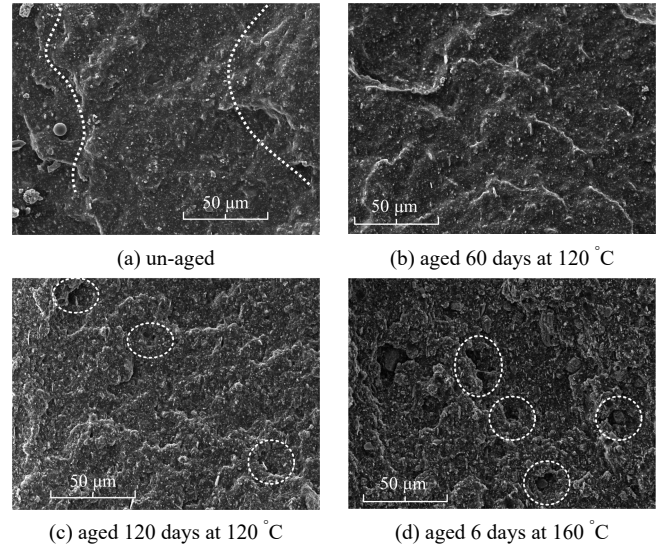


Figure 8. Cross section of EPR aged at 120 and 160 °C.

Since EPR contains some chemical products, such as dicyclopentadiene (DCPD), ethylidene norbornene (ENB) and vinyl norbornene (VNB), which contributes to the formation of cross-links, amorphous and complex structures. For charge injection and transport, some trap sites can be formed by this chemical groups or structures. As shown in Figure 3 and 4, the appearance of the heterocharge near the anode mainly results from the by-products during the thermal ageing.

Considering the change of the molecular structure of EPR as shown in Figure 9, the oxidation reaction occurs mostly in the propylene chain segment. The tertiary carbon atom with the side methyl is much active and easy to form hydroperoxide through dehydrogenation under thermal stress. Then the polar hydroxyl group comes from the homolysis of hydroperoxide, which is the main polar group in the EPR and will migrate or neutralize with electron or negative ions [22]. The rate of thermal oxygen action will increase with the rise of temperature and the ageing time [23], and the formation, migration and neutralization of space charges will be much more active, namely the change and development of trapping and de-trapping of the space charge at all time, which results in the difference of the space charge characteristics under different ageing process.

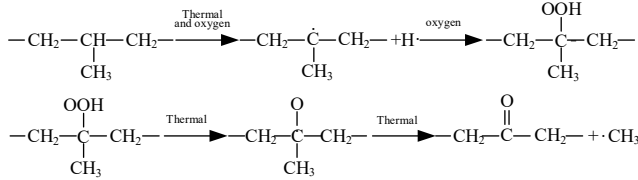


Figure 9. Effect of the thermal stress on the structure of EPR.

4.3 DISTRIBUTION OF TRAP ENERGY DURING THERMAL AGEING

Local states distributing in the energy levels of EPR are called as traps. The space charge caused by the injection from electrodes or the ionization of impurities migrates into the sample through trapping and de-trapping, so the space charge behavior characteristics can reflect the distribution of the trap and is used to explore the influence of the thermal stress on the distribution of the space charge. Isothermal decay current (IDC) method is a mature method used to the study of trap energy of organic solid [24]. However, the current density cannot be obtained by measuring the space charge, so the surface potential is used for an intermediary to find the relationship between the space charge and current density.

The relationship between surface potential $V_s(t)$ and current density $j(t)$ in decay process can be expressed as:

$$j_{\text{decay}}(t) = C \frac{dV_s(t)}{dt} \quad (5)$$

$$C = \varepsilon_0 \varepsilon_r A / L \quad (6)$$

where C is the equivalent capacitance of the sample, A and L are surface area and thickness of sample respectively. The relationship between surface space charge density and surface potential V_s is:

$$\sigma(t) = \varepsilon_0 \varepsilon_r V_s(t) / r' \quad (7)$$

where r' is the mean charge depth which takes 120 pm. The dissipation characteristic of space charge density can be fitted as an exponential decay law as mentioned before, so the relationship between decay current density and charge density of space charge during dissipation can be obtained by Equations (4) to Equation (7) as:

$$|j_{\text{decay}}(t)| = \frac{r'}{L} \frac{A}{\tau} e^{-t/\tau} \quad (8)$$

The trap level, E_t , and trap energy density, $N(E_t)$, can be calculated by:

$$E_t = kT \ln \nu t \quad (9)$$

$$j_{\text{decay}}(t) = \frac{qLkT}{2t} f_0(E_t) N(E_t) \quad (10)$$

where k is Boltzmann's constant, which is 8.568×10^{-5} eV/K, T is absolute temperature, ν is vibration frequency of electron, which is 3×10^{12} s⁻¹.

The trap energy properties of the EPR is shown in Figure 10. In the 120 °C ageing process, the trap depth increases obviously at aged for less than 30 days and the maximum value is 0.92 eV, while the increment of trap density is small. It shows that the “degassing process” as mentioned before mainly increases the trap depth. After EPR is aged for 60 days, the trap density increases obviously, but the trap depth corresponding to the maximum trap density is about 0.90 eV, which is smaller than that of EPR aged for 30 days. At the end of life of EPR, both the trap depth and trap density are decreased. Based on the judgments of the space charge behavior in EPR during thermal ageing as mentioned in 3.1 and the theory of “trap filling”, the rapid enhancement of electrode injection increases the space charge density in the sample. The more the sample closes to the end of life, the more the relative deep trap is gradually filled up, and the more difficult the charge captured by deep traps dissipates. Then the mobility increases and the trap depth decreases in this stage. It is the reason why a little of space charge accumulates inside the EPR sample both at the beginning or the end of life under the thermal ageing.

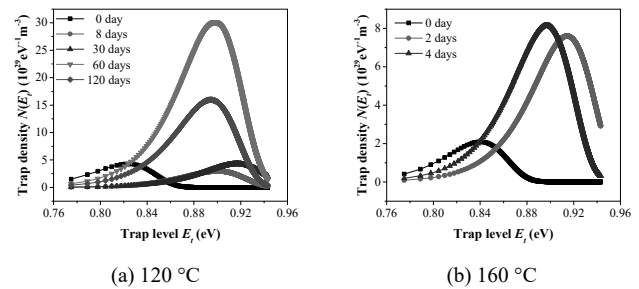


Figure 10. Trap distribution of EPR aged at 120 °C and 160 °C.

Under 160 °C thermal ageing, the trap depth of the maximum trap density is about 0.91 eV when sample is aged for 2 days. The trap density reaches maximum when sample is aged for 4 days. It can be found that the trend of the trap density with ageing time under 160 °C thermal ageing is different from that under 120 °C thermal ageing. It can be ascribed to the severe thermal damage in short time which make the molecular chain break rapidly and lead to a significant increase of trap density.

5 CONCLUSION

Thermal stress endurance tests were carried out on the film samples of EPR at 120 and 160 °C respectively. The effects of the thermal stress on the space charge characteristics and the physicochemical properties were discussed.

(1) The higher the ageing temperature, the shorter the life of EPR. The space charge characteristics is also different under lower and higher ageing temperature. Based on the charge polarity near the anode, the space charge profile in the 120 °C ageing process can be divided into three stages, which are homocharge (un-aged), heterocharge (at the early ageing stage) and homocharge (at the middle and later ageing stage). In the 160 °C ageing process, there is heterocharge accumulated near the electrodes and positive charge accumulated at inner sample until the end of life once the ageing began.

(2) The oxidation reaction during the thermal ageing forms the layers and compact microspores in EPR. The EPR molecular chain break makes the polar groups and ions increase. The complex changes of physical and chemical structures during thermal ageing are the main reasons for the increase of complex permittivity as well as the change of trap distribution.

(3) Based on the decay data of space charge in EPR and IDC theory, the distribution of trap levels at different ageing stages is obtained. The trap depth first increases and then decreases with ageing time. The dividing point of ageing time, at which the trap level rises to the maximum, is 60 days at 120 °C and 2 days at 160 °C. Based on the theory of trap filling, the increase of carrier density and charge injection induces more deep traps in EPR before the dividing point. After the dividing point, the deep trap is filled and the carrier mobility increases gradually, which make the trap density decrease.

ACKNOWLEDGMENT

Project supported by National Natural Science Foundation of China (51577123, U1510112, 51377113), Natural Science Foundation of Shanxi Province (201601D021092, 201601D202052) and Youth Foundation of Taiyuan University of Technology (1205-04020202).

REFERENCES

- [1] K. Matsui, Y. Tanaka, T. Takada, T. Fukao, K. Fukunaga, T. Maeno, and J. M. Alison, "Space charge behavior in low density polyethylene at pre-breakdown," *IEEE Trans. Dielectr. Electr. Insul.*, vol. 12, no. 3, pp. 406–415, 2005.
- [2] Y. Sekii, and T. Maeno, "Generation and Dissipation of Negative Heterocharges in XLPE and EPR," *IEEE Trans. Dielectr. Electr. Insul.*, vol. 16, no. 3, pp. 668–675, 2009.
- [3] C. Y. Li, C. J. Lin, J. Hu, W. D. Liu, Q. Li, B. Zhang, S. He, Y. Yang, and J. L. He, "Novel HVDC Spacers by Adaptively Controlling Surface Charges-Part I: Charge Transport and Control Strategy," *IEEE Trans. Dielectr. Electr. Insul.*, 2018.
- [4] C. Y. Li, C. J. Lin, Y. Yang, B. Zhang, W. D. Liu, Q. Li, J. Hu, S. He, X. L. Liu, and J. L. He, "Novel HVDC Spacers by Adaptively Controlling Surface Charges-Part II: Experiment," *IEEE Trans. Dielectr. Electr. Insul.*, 2018.
- [5] T. J. Lewis, "Ageing-a perspective," *IEEE Electr. Insul. Mag.*, vol. 17, no. 4, pp. 6–16, 2001.
- [6] J. Li, B. Du, Y. Xing, and J. Jin, "Trap Distribution and Flashover Characteristics of Carbon-Black-Filled EPDM in Low Temperature," *IEEE Transactions on Applied Superconductivity*, vol. 26, no. 7, pp. 1–5, 2016.
- [7] J. Li, B. X. Du, X. X. Kong, and Z. L. Li, "Nonlinear conductivity and interface charge behaviors between LDPE and EPDM/SiC composite for HVDC cable accessory," *IEEE Transactions on Dielectrics & Electrical Insulation*, vol. 24, no. 3, pp. 1566–1573, 2017.
- [8] A. Imburgia, R. Miceli, E. R. Sanseverino, P. Romano, and F. Viola, "Review of space charge measurement systems: acoustic, thermal and optical methods," *IEEE Trans. Dielectr. Electr. Insul.*, vol. 23, no. 5, pp. 3126–3142, 2016.
- [9] C. Y. Li, J. Hu, C. J. Lin, and J. L. He, "The potentially neglected culprit of DC surface flashover: electron migration under temperature gradients," *Sci. Rep.*, vol. 7, no. 1, pp. 3271, 2017.
- [10] C. Guo, Y. Zhang, F. Zheng, Z. An, Z. Zhu, L. Yang, J. Zhang, and E. Yu, "Comparison of space charge distribution measurements among planar sample, HVDC Cable on external layer and from inner conductor by Laser PWP method," *Int. Conf. Electr. Mat. Power Equip.*, 2017, vol. 1, pp. 461–463.
- [11] M. Abou-Dakka, S. Bamji, and A. Bulinski, "Space charge distribution measurements in XLPE and EPR," *Annu. Rep. Conf. Electr. Insul. Dielectr. Phenom. (CEIDP)*, 1997, vol. 1, pp. 23–27.
- [12] H. Q. He, X. Wang, S. J. Liu, M. S. Cui, and D. M. Tu, "Space Charge in EPR Insulator in Different Elongations," *Insul. Mater.*, vol. 39, no. 5, pp. 40–44, 2006. (in Chinese).
- [13] Y. Liu, H. Liu, L. Yu, Y. Li, and L. Gao, "Effect of thermal stress on the space charge distribution of 160 kV HVDC cable insulation material," *IEEE Trans. Dielectr. Electr. Insul.*, vol. 24, no. 3, pp. 1355–1364, 2017.
- [14] L. Cao, and S. Grzybowski, "Life-time characteristics of EPR cable insulation under electrical and thermal stresses," *IEEE Int. Conf. Solid Dielectr. (ICSD)*, 2013, vol. 1, pp. 632–635.
- [15] C. Stancu, P. V. Notingher, P. Notingher, and M. Lungulescu, "Space charge and electric field in thermally aged multilayer joints model," *IEEE Trans. Dielectr. Electr. Insul.*, vol. 23, no. 2, pp. 633–644, 2016.
- [16] H. Uehara, G. C. Montanari, Q. Chen, Z. Li, and Y. Cao, "Comparison of space charge behavior in XLPE and EPR with thermal gradient," in *IEEE Int. Conf. Dielect. (ICD)*, 2016, vol. 1, pp. 143–146.
- [17] J. Li, B. X. Du, and H. Xu, "Suppressing interface charge between LDPE and EPDM for HVDC cable accessory insulation," *IEEE Trans. Dielectr. Electr. Insul.*, vol. 24, no. 3, pp. 1331–1339, 2017.
- [18] W. Wang, Y. Tanaka, T. Fujitomi, T. Takada, and S. Li, "Study on conduction current and space charge accumulation simultaneously in Ethylene Propylene Diene Monomer film," *Int. Conf. Electr. Mat. Power Equip.*, 2017, vol. 1, pp. 464–467.
- [19] C. Stancu, P. V. Notingher, L. Dumitran, L. Taranu, A. Cernat, and A. Constantin, "Thermal ageing effect on the DC cable joints insulations," *Int. Conf. Appl. Theoretical Electricity*, 2016, vol. 1, pp. 1–6.
- [20] T. Takada, Y. Tanaka, N. Adachi, and Q. Xiaokui, "Comparison between the PEA method and the PWP method for space charge measurement in solid dielectrics," *IEEE Trans. Dielectr. Electr. Insul.*, vol. 5, no. 6, pp. 944–951, 1998.
- [21] J. Hao, "Study on Time/Frequency Domain Dielectric Spectroscopy and Space Charge Characteristics of Transformer Oil-Paper Insulation Thermal Aging," PhD dissertation, Chongqing University, 2012.
- [22] R. Sundarajan, A. Mohammed, N. Chaipanit, T. Karcher, and Z. Liu, "In-service aging and degradation of 345 kV EPDM transmission line insulators in a coastal environment," *IEEE Trans. Dielectr. Electr. Insul.*, vol. 11, no. 2, pp. 348–361, 2004.
- [23] T. Tanaka, "Aging of polymeric and composite insulating materials. Aspects of interfacial performance in aging," *IEEE Trans. Dielectr. Electr. Insul.*, vol. 9, no. 5, pp. 704–716, 2002.
- [24] K. Yang, N. Zheng, G. J. Zhang, M. Dong, and Z. Zhang, "Analysis of Surface Trapping Parameters of Solid Insulation Dielectrics," *High Volt. Eng.*, no. 9, pp. 13–16, 2007. (in Chinese).



Rujia Men received the B.Sc. degree and the M.Sc. degree from the Taiyuan University of Technology, China in 2007 and 2010, respectively. She joint Shanxi State Owned Huanqiu Engineering Co., Ltd. as the electrical engineering from 2010 to 2015. Now, she is pursuing her Ph.D. degree in the Taiyuan University of Technology. Her main research interest is the condition assessment of electrical equipment and power system analysis.



characteristics, intelligence techniques in coal mine.

Zhipeng Lei (M'13) received the B.Sc. degree from the East China Jiaotong University, China in 2005, and the M.Sc. degree, Ph.D. degree from the Taiyuan University of Technology, China in 2010 and 2015, respectively. He joined the College of Electrical and Power Engineering in the Taiyuan University of Technology as a lecturer since 2015. He is now a post-doctor in University of Bologna. His main research interest is the condition assessment of high voltage cable failure and associated partial discharges



He has performed a number of electrical failure investigations about coal mine. He has presented a number of technical and scientific papers at international conferences and seminars.

Jiancheng Song (M'13) received the B.Sc. degree from Taiyuan University of Technology, China, in 1982, the M.Sc. degree from Newcastle University, England, in 1987, respectively and the Ph.D. degree from Xi'an Jiaotong University, China, in 1999. Currently, he is a professor of the College of Electrical and Power Engineering at Taiyuan University of Technology. He has experience in the field of condition assessment, remaining life assessment and intellectual automation technology.



Davide Fabiani (M'98 SM'16) received the M.Sc. and Ph.D. in Electrical Engineering with honours in 1997 and 2002, respectively. He is Associate Professor at the Department of Electrical Electronics and Information Engineering of University of Bologna. His fields of research are mainly related to development, characterization and diagnosis of electrical insulation systems for applications in electrical and electronic apparatus. He is author or co-author of about 180 papers, most of them published on the major international journals and conference proceedings. He is Associate Editor of the Transactions on Dielectrics and Electrical Insulation and IET High Voltage Journal. He is currently member of DEIS AdCom and Chair of the Meetings Committee since 2016.